Comp. Biochem. Physiol. Vol. 93A, No. 4, pp. 685–690, 1989
Printed in Great Britain

0300-9629/89 $3.00 + 0.00
© 1989 Maxwell Pergamon Macmillan plc

INTRACELLULAR ELECTRICAL POTENTIALS AND MEMBRANE RESISTANCES OF THE DUODENAL EPITHELIUM IN THE LIZARD, *GALLOTIA GALLOTI*

T. GÓMEZ, A. LORENZO and F. GIRALDEZ*

Depto. Biología Animal, Universidad de La Laguna, 30005 Tenerife, Spain; and *Depto. Bioquímica y Biología Molecular y Fisiología, Universidad de Valladolid, Spain

(*Received* 22 *December* 1988)

Abstract—1. The cellular electrophysiological properties of the small intestine epithelium of the lizard *Gallotia galloti* were studied with microelectrodes and conventional electrophysiological techniques.

2. The average intracellular potential difference was 30.5 mV cell negative, with respect to the mucosal solution and 32.5 mV cell negative with respect to the serosal solution.

3. The transmural potential (E^t) was 1.56 mV (mucosa negative) and the equivalent short-circuit current (I_{sc}) was 11.7×10^{-6} A/cm^2.

4. The fractional resistance of the luminal membrane (fR^m) was 0.45 indicating that transcellular resistance to current flow is distributed approximately equally between the luminal and the serosal membranes.

5. The ratio of the junctional resistance to the transcellular resistance pathway ($R^j/R^m + R^s$) was 0.06.

6. Substitution of Na in the luminal solution by either K or choline led to a small change in E^t (< 1 mV), and a 5 mV change in E^m. Chloride removal depolarized the luminal membrane by 16.8 mV.

7. These results indicate that, across the apical membrane, $P_k > P_{cl} > P_{Na}$. The tight junctions are poorly selective to ions.

8. Glucose, alanine and phenyalanine, at transport saturating concentrations, reversibly depolarized the luminal membrane.

INTRODUCTION

The mechanisms responsible for the transport of ions and non electrolytes by the small intestine have been extensively studied during the last few years. Active transport of sugars, amino acids and other substrates across the intestinal mucosa is now well characterized in different species of mammals (Paterson *et al.*, 1979; Kaunitz *et al.*, 1982; Kimmich, 1981; Fromter, 1982), birds (Suarez and Lorenzo, 1982; Kimmich and Randles, 1984; Grubb *et al.*, 1987), amphibia (Gunter-Smith *et al.*, 1982) and fish (Albus *et al.*, 1983) where cellular models of substrate transport are based on flux measurements and electrophysiological studies. Recent work done on the lizard *Gallotia galloti* has extended these studies to reptilia where the basic kinetic properties of galactose and phenylalanine transport are now available (Gómez *et al.*, 1986; Bolaños *et al.*, 1986). The purpose of the present work has been to study the cellular electrophysiological properties of the small intestine of a lacertid, the lizard *Gallotia galloti*, on which to our knowledge, there is no information available. We report here the basic electrical potential profile and parameters of a stripped preparation of lizard duodenal epithelium as well as some observations on the cell and transepithelial responses to changes in the composition of the luminal solution. Circuit analysis was employed to work out the basic properties of the different permeation pathways. The results compare well with those obtained in other animal species showing the basic pattern of cell membrane polarization in parallel with a highly conductive paracellular pathway.

MATERIALS AND METHODS

Lizards (*Gallotia galloti*) were captured at Hoya Fria (Tenerife) and kept in a terrarium until required. They were captured in the last days of November and the experiments performed in Valladolid in December. Animals were killed and the duodenum removed and then rinsed and placed on a Petri dish covered with Sylgard where the epithelium was mechanically stripped of the underlying muscular layers by dissection with forceps under the microscope. The tissue was then mounted, mucosa upwards, in a modified Ussing chamber suitable for microelectrode studies (Giraldez, 1984). The exposed area of epithelium was 0.2 cm^2. The mucosal side was bathed by a thin layer of solution flowing under gravity, which could thus be changed in less than 10 sec. The solution in the lower chamber (serosal) was periodically renewed. The standard bathing solution (normal Ringer) had the following composition (mM): Na^+, 136; K^+, 4.5; Ca^{2+}, 1.3; Mg^{2+}, 1; Cl^-, 114; CO_3H^-, 25, buffered to a pH of 7.4 with 5 mM Hepes–Tris and 2 mM $H_2PO_4/NaHPO_4$. The Na concentration of the mucosal bathing solution was reduced in some experiments by isotonic replacement with the appropriate gluconate salts and increasing the Ca^{2+} concentration to 10 mM to account for the decrease in Ca^{2+} activity in the presence of gluconates. In experiments, alanine, phenylalanine or glucose were added to a final concentration of 20 mM. In these cases a fraction of NaCl was replaced by the corresponding amount of substrate to achieve final isotonicity.

The experimental set-up and the electrical arrangements are illustrated in Fig. 1A. Microelectrodes were made from borosilicate glass tubing, 1.2 mm o.d., and had resistances of about 70 MΩ when filled with 3 M KCl and measured in Ringer. Electrodes were usually bevelled or broken throughout the experiments and tips corresponding to microelectrode resistances of about 30 MΩ were most successfully

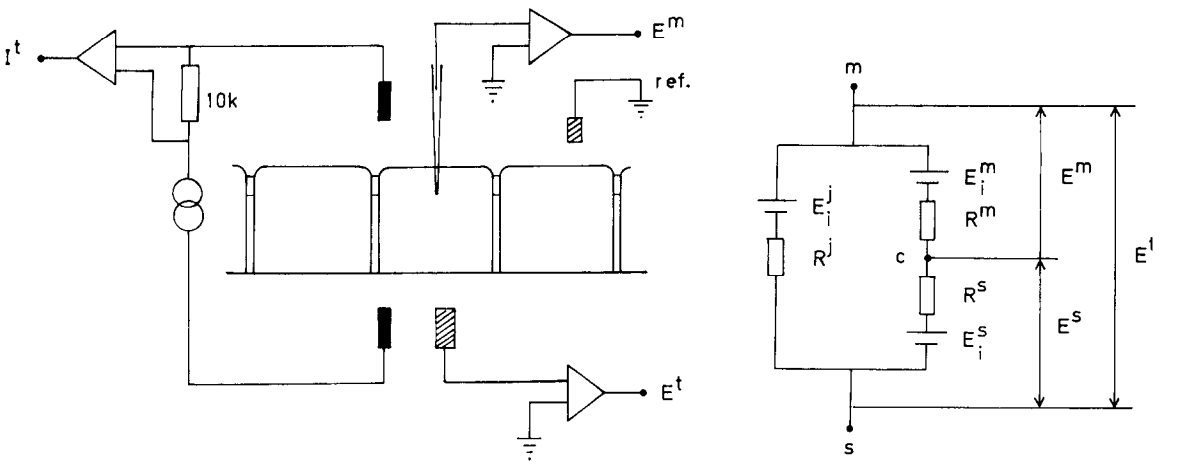

(A) (B)

Fig. 1.(A). Experimental set-up and electrical arrangements for recording membrane potentials and resistances in small intestine epithelium. The mucosal fluid was continuously perfused by fluid running under gravity and collected by a suction pipette. The composition of the bathing solution could be changed in less than 10 sec by operation of a multi-way valve. Cells were impaled from the mucosa and potentials referred to both reference electrode located in the mucosal bath which was grounted. Transepithelial current was injected through two Ag: AgCl electrodes and measured as the voltage drop across a 10 Ω resistor. (B) Steady-state equivalent circuit for duodenal epithelial cells. Symbols refer to: E_i. lumped electromotive forces, E, recorded potentials, R, resistances. Superscripts m, s, j refer to mucosal, serosal and junctional.

employed. The signal from the microelectrode was monitored by a voltage-follower with bridge-balance and capacity compensation facilities. Bath electrodes were made with 2% 3 M KCl agar bridges connected through AgCl:Ag half cells. Square wave current pulses, 100 μA/cm^2, were passed between mucosa and serosa through AgCl electrodes from a floating current source. The current was measured by the voltage drop across a 10 Ω resistor with a differential amplifier. Mucosal bath was grounded. Symbols and sign conventions followed here for the different potentials are as follows: E^m and E^s were referred to the cell, and are apical and basal membrane potentials respectively; E^t is the transepithelial potential. Results were analysed according to the equivalent electrical circuit shown in Fig. 1B. $E_i^{m,t,j}$ represent the lumped electromotive forces across each barrier m, s, or j, and $R^{m,s,j}$ the corresponding, lumped resistances. The resistance transepithelial (R^t) was calculated from the voltage deflection in response to transepithelial current pulses:

$$R^t = \frac{E^t}{I^t}. \tag{1}$$

The fractional resistance of the mucosal membrane fR^m was calculated from the transepithelial voltage deflections and those recorded across the mucosal barrier with the microelectrode within the cell:

$$fR^m = \frac{R^m}{R^m + R^s} = \frac{E^m}{E^t}. \tag{2}$$

According to the circuit in Fig. 1B, the value of R^t is:

$$R^t = \frac{(R^m + R^s)\,R^j}{R^m + R^s + R^j}. \tag{3}$$

The general solution of the circuit in Fig. 1B for E^m, E^s and E^t is:

$$E^m = \frac{E_i^m\,(R^s + R^j) + R^m(E_i^s - E_i^j)}{R^m + R^s + R^j} \tag{4}$$

$$E^s = \frac{E_i^s(R^m + R^j) + R^s(E_i^m + E_i^j)}{R^m + R^s + R^j} \tag{5}$$

$$E^t = \frac{R^j(E_i^s - E_i^m) + E_i^j(R^m + R^s)}{R^m + R^s + R^j}. \tag{6}$$

According to equations (4)–(5), it is possible to calculate E_i^m and E_i^s if the resistances and the potential across the cell membranes and the entire epithelium are known:

$$E_i^m = E^m - E^t\frac{R^m}{R^j} \tag{7}$$

$$E_i^s = E^s + E^t\frac{R^s}{R^j}. \tag{8}$$

RESULTS

General electrophysiological properties in Ringer solution

The following experiments show the measurement of the intracellular electrical potentials and membrane resistance of epithelial cells using microelectrodes, as described in the Materials and Methods. A diagram of the preparation is shown in Fig. 1B and a typical recording of E^m and E^t is shown in Fig. 2. The record starts with the microelectrode in the mucosal bath where the impedance of the microelectrode was measured. At the arrow the cell is impaled as recognized by the sudden negative-going change in the potential and the increase in the electrode resistance, upward deflections (see below). The potential was stable within a few mV throughout the period of the measurements and returned to the original baseline level of the mucosal bath upon withdrawal of the electrode. At the same time the microelectrode resistance was restored to its initial value. Negative-going pulses during the penetration were caused by cell transepithelial current pulses that were applied to measure the transmural resistance (R^t) and the frac-

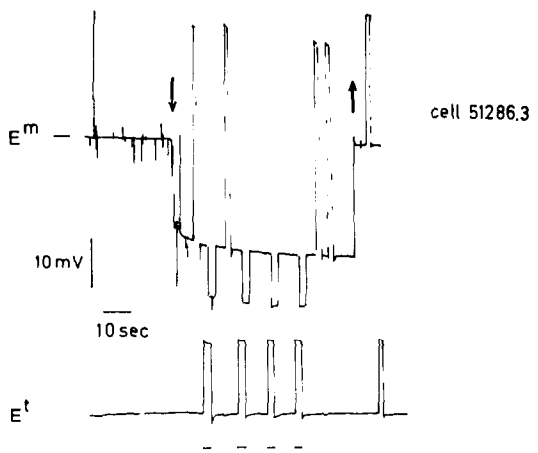

Fig. 2. Recording of intracellular potential and transepithelial potential in duodenal epithelium of the lizard. The upper trace shows cell membrane potential, E^m, recorded with a microelectrode and the lower trace the transepithelial potential, E^t. Penetration and withdrawal of the microelectrode are indicated by the arrows. Upward deflections in the upper trace correspond to 1 nA current pulses injected through the microelectrode to monitor microelectrode and cell resistances. Downward deflections correspond to transmural current pulses and were used to monitor fractional resistances.

tional resistance of the mucosal membrane (fR_m) as described in the Materials and Methods. Conventional impalement criteria are seen to be fulfilled here; (a) sharp deflection on entry, (b) stability of the recorded potential, (c) absence of changes in electrode tip-potential, (d) constancy of fractional resistance and (e) moderate increase in the microelectrode resistance.

The results of several experiments done in steady-state with both sides of the epithelium bathed in Ringer solution are summarized in Tables 1 and 2. The average intracellular potential was about 30 mV cell negative with respect to mucosa, ranging from 25 to 37 mV. The value of fR_m (0.44 ranging from 0.2 to 0.8) indicates that the resistance to current flow is distributed equally between the luminal and the serosal membranes. The equivalent short-circuit current can be calculated from E^t and R^t and becomes 11.7×10^{-6} A/cm^2, in agreement with previous work done on this tissue (Gómez *et al.*, 1986).

As shown in Fig. 2, current pulses through the microelectrode, 1 nA, revealed an increase in the apparent electrode resistance inside the cell. That this reflected the input resistance of the cell was corroborated by inspection of the time course of the voltage trace in the oscilloscope after electronic balance and compensation of the microelectrode resistance and capacitance. The average microelectrode increment

Table 1. Transepithelial potentials of the isolated lizard duodenal epithelium in steady-state and Cl substitution in the mucosal solution

Mucosal solution	n	E^m (mV)	E^s (mV)	E^t (mV)
Control	(18)	30.5 ± 2.8	32.1 ± 2.8	1.56 ± 0.21
Cl free	(6)	10.16 ± 3.6*	30.1 ± 1.6	19.9 ± 2.68*

Values are the mean ± SEM; n, number of experiments.
*Significant difference $P < 0.001$, respectively, with the control series according to the t-test.

resistance measured in this way was of 32.5 MΩ (shown in Table 2), and can be taken as a lower estimate for the cell input resistance since lateral spread of current through intracellular functions is likely to occur. This value corresponds to that of $R^m \times R^s/R^m + R^s$ (see circuit in Fig. 1B). Keeping in mind that we are ignoring the lateral spread of current, we can obtain from these data the estimated value for each cell membrane specific resistance. Light microscopy revealed that the epithelial cells of lizard duodenum are long but narrow (7–15 μm wide, 35–45 μm deep). For a cell of about 40 μm in height and 10 × 10 μm in width the value of R^m and R^s is 1037 and 1346 Ω cm^2, respectively(Table 2). From equation (3) we obtain a value for R^j of 140.6 Ω cm^2. The ratio of the junctional resistance, R^j to that of the transcellular pathway proves to be 0.06. Equation (5) can now be easily solved assuming that in the steady stated, with symmetric solutions, $E_1^j = 0$. Then equation (6) simply becomes: $E^t = 0.06 \times (E_1^s - E_1^m)$. For $E^t = +1.56$, the difference $E_1^s - E_1^m$ is 26 mV.

The equivalent electromotive forces across each individual membrane were also calculated in these experiments from the values of potentials and resistances, using equations (4)–(8) and under the assumption that with symmetric solutions $B^j = 0$. The results are summarized in Table 3. It can be seen that both mucosal and serosal EMFs are oriented so as to make the cell interior negative. They are not symmetric and the difference $E_1^s - E_1^m$ is about 30 mV, very close to the value calculated above. This asymmetry generates a current that flows through the junctional pathways, tending to collapse the difference.

Luminal replacements

The effects of changing the luminal concentration of the major monovalent ions, Na^+, K^+ and Cl^- are illustrated in Fig. 3. Here, the composition of the luminal bath was changed, as indicated at the bottom, while continuously monitoring E^m and fR^m. The striking feature of the records for Fig. 3 is the large fast depolarization induced by Cl^--free solutions, in contrast with the lack of effect of replacing Na^+ by K^+. Four experiments in which Na^+ was replaced by either K^+ or choline produced changes in E^m and E^t that were 5 mV and 1 mV, respectively. The effects of Cl^--removal were studied more extensively and the results of several experiments are summarized in Tables 2 and 3. It can be seen that the absence of Cl^- produced a depolarization of the luminal membrane of 16.8 mV that was accompanied by an increase in fR^m of about 15%. The transmural potential, E^t, also changed, making the epithelium hyperpolarized (mucosa more negative). E^s remained almost unchanged after luminal zero Cl^-, ($E^s = 29.2$ mV in Ringer and 30.06 mV in zero Cl^-). The results were further analysed using equations (4)–(8) of the Materials and Methods section.

Assuming that E^s remains constant after a change in the luminal bathing solution, the imposed change in the luminal EMF after the perturbation can be calculated from:

$$E_1^m(2-1) = \frac{E_2^m}{fR_2^s} - \frac{E_1^m}{fR_1^s} + \alpha_2 E_2^j + E_1^s(\alpha_1 - \alpha_2), \quad (9)$$

Table 2. Resistances of the cell membranes (R^m, R^s, R^t), shunt (R^j) and the apparent microelectrode input resistance (R^i) and fractional resistance of the mucosal membrane (fR^m) in steady state and on the Cl^- substitution in the mucosal solution

Mucosal solution	n	$R^m(\Omega cm^2)$	$R^s(\Omega cm^2)$	$R^t(\Omega cm^2)$	$R_i(\Omega cm^2)$	$R_i(M\Omega)$	fR^m
Control	(18)	1037 ± 93.1	1346 ± 239	133 ± 11	140.6 ± 0.8	32.5 ± 5.1	0.44 ± 0.04
CL free	(6)	1584 ± 230*	802 ± 127	1322 ± 18	140.8 ± 0.49	31.3 ± 7.0	0.75 ± 0.06†

Values are the mean ± SEM, n number of experiments. *, † significant difference $P < 0.05$ and $P < 0.001$, respectively, with the control series according to the t-test.

where superscripts 1 and 2 refer to the original and the experimental condition and α is the ratio $R^m/R^s = fR^m/fR^s$. The change in E_t^m after zero Cl^- is of -28.8 ± 3.75 mV and the relative permeabilities of the luminal membrane are P_K: P_{Na}: $P_{Cl} = 1$: 0.3: 0.88.

The analysis of the selectivity of the junctional pathways is much simpler because of the high value of the ratio $(R^m + R^s)/R^j$, that makes $E^j = E^t$. The permeability ratios were then directly computed from the GHK equation. The values were P_K: P_{Na}: $P_{Cl} = 1$: 0.78: 0.89, making the junctional pathways poorly selective to ions.

Finally, the effects of some known substrates for active transepithelial transport were also measured in five experiments. Glucose, alanine and phenylalanine, at saturating concentrations, were effective in depolarizing the luminal membrane. The size of the depolarization varied from cell to cell and for each substrate ranging from 3 to 20 mV. This is clearly illustrated in the reponses to glucose and alanine shown in Fig. 3. The effects of 20 mM glucose, at the beginning of the recording (to the left) and 20 mM alanine, at the end, are shown. It can be noticed that, in both cases, despite the differences in the size of the responses, the effect consists of a luminal cell membrane depolarization that was reversible upon removal of the actively transported substrate. No clear change could be measured in the fractional membrane resistances. the transmural potential (E^t) increased during substrate load with a concomitant net increase in the equivalent short-circuit current. This increase ranged from 22.5×10^{-6} A/cm^2 to 150×10^{-6} A/cm^2.

DISCUSSION

The experiments reported here were aimed at studying the basic electrical properties of the duodenal epithelium of the lizard. The results show that the electrical potential profile is that of a typical "leaky" epithelium with a large conductance paracellular pathway. The selectivity of the luminal membrane to monovalent ions is poor. The effect of actively transported substrates is to depolarize the cell membrane in concomitance with an increase in the short-circuit current.

Table 3. Equivalent electromotive forces at both cell borders

Cell membrane	Measured potential (mV)	Equivalent EMF (mV)	Difference (mV)
Apical	30.5 ± 2.8	16.23 ± 2.9	14.27 ± 0.96
Basolateral	32.1 ± 2.8	46.33 ± 4.19	-13.43 ± 1.18

Ringer's on both sides, $n = 18$ preparations. Polarities defined in Materials and Methods section.

Previous works using the transepithelial voltage-clamp technique (Gómez *et al.*, 1986; Bolaños *et al.*, 1986) have also shown that the lizard duodenum behaves like a "leaky" epithelium, exhibiting a low transmural resistance, about 100 Ω cm^2. The present study confirms these measurements and shows that about 90% of this conductance is located in the paracellular pathway. These values and the general electrical pattern are very similar to those reported for the small intestine of other animal species such as rabbit ileum (Rose and Schultz, 1971), rat jejunum (Munck, 1972), humam ileum (Al-Awqati *et al.*, 1973; Grady *et al.*, 1967) and *Necturus* small intestine (Giraldez *et al.*, 1988). These tissues are characterized by a low spontaneous transepithelial electrical potential difference, low transepithelial resistance and high hydraulic conductivity. These properties are known to be associated to a high capacity for water transport, hence in the lizard, fluid transfer across the intestine could contribute to reulate osmotic equilibrium.

Comparison of values of electromotive forces and potentials across each membrane indicates the dominance by K^+ of the basolateral membrane potential and a poor selectivity to ions of the luminal barrier. Ion substitution experiments also suggest a slight selectivity of the apical membrane for cations. This is similar to what happens in *Necturus* enterocytes when they are not stimulated by cAMP and a large Cl-conductance is activated (Giraldez *et al.*, 1988).

Figures obtained for individual membrane resistance, although rough estimates, give values that are too high to accommodate transepithelial Na^+ fluxes. A resistance of about 1000 Ωcm^2 would allow a current of 30×10^{-6} A/cm^2. For the ratio of mucosal permeabilities calculated in the Results, the corresponding value for the maximal Na^+ current would be about 9×10^{-6} A/cm^2 which is a 30% of the mucosal current. Our estimates of the cell input resistance ignore the lateral spread of current. This observation is in agreement with studies done in one of our laboratories (Lorenzo *et al.*, in press) showing that the entry of sodium into the cell across the luminal membrane occurs by two pathways. Fifty percent of the Na^+ influx occurs through the Na^+/H^+ antiport and the other part through an electrogenic conductive pathway. The second pathway may be responsible for the serose-positive of the PD under standard conditions. The chloride ions enter across the brush border membrane in exchange for bicarbonate. Following this model, the electrogenic Na^+ influx across the mucosal membrane was 8.84×10^{-6} A/cm^2 (Gómez *et al.*, 1986) Sugar and amino acid absorption have been studied only in a few specimens of reptilia (Wright, 1986; Gilles-Baillien, 1967; Lamsfus 1976). Tracer and short-circuit

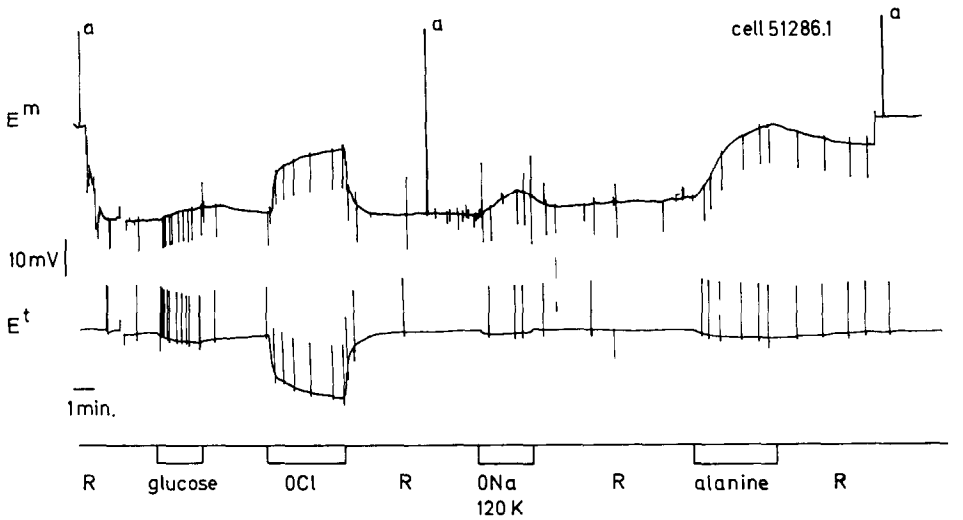

Fig. 3. Effects of ions and actively transported substrates on cell and transepithelial membrane potentials. Cell membrane potential, upper trace, and transepithelial potential, lower trace, were continuously monitored during changes in the composition of the mucosal bathing solution. Changes are indicated at the bottom. The standard solution is indicated by R, glucose, alanine, chloride-free (0Cl) and Na for K substitutions (0Na, 120K) were carried out as described in the Materials and Methods section.

studies performed on lizard intestine (Gómez *et al.*, 1986; Bolaños *et al.*, 1986) indicate that the properties of galactose and phenylalanine transport in the lizard are similar to those described in mammals and birds. Galactose and phenylalanine are transported against a concentration gradient and this transport is fully dependent on sodium and accompanied by an increase in the short-circuit current. The cellular electrical events associated with the transport of these substrates appear to involve a cell depolarization with little change in conductance which is consistent with the notion that transport of substrates occurs as a secondary active process coupled to the influx of Na^+. The substrate dependent Na^+ current generated in this way would produce the depolarization of the luminal cell membrane and a new steady-state potential closer to the Na^+ equilibrium potential.

Acknowledgements—This research was supported by Grant no. 3037 from the Spanish Government Agency CAICYT. The authors wish to thank the engineer Francisco Carrasco for his helpful advice on the electrical models.

REFERENCES

Al-Awqati Q, Cameron J. L. and Greenough W. B. (1973) Electrolyte transport in human ileum: effect of purified cholera exotoxin. *Am. J. Physiol.* **224,** 818–823.

Albus H. Bakker R. and Siegenbeek van Heukelom J. (1983) Circuit analysis of membrane potential changes due to electrogenic sodium dependent sugar transport in goldfish intestinal epithelium. *Pflügers Arch.* **398,** 1–9.

Bolaños A., Gómez T. Badía P. and Lorenzo A. (1986) Electrical properties of a Na-dependent phenylalanine transport in lizard (*Lacerta galloti*) *duodenum. Comp. Biochem. Physiol.* **84A,** 405–408.

Fromter E. (1982) Electrophysiological analysis of rat renal sugar and amino acid transport. I. Basic phenomena. *Pflügers Arch.* **393,** 209–224.

Gilles-Baillien M. and Schohheniels E. (1967) Bioelectrical potentials in the intestinal epithelium of the Greek tortoise. *Comp. Biochem. Physiol.* **23,** 95–104.

Giraldez F. (1984) Active sodium transport and fluid secretion in the gallbladder epithelium of *Necturus. J. Physiol.* **348,** 431–455.

Giraldez F., Sepulveda F. V. and Sheppard D. N. (1988) A chloride conductance activated by adenosine 3′-5′-cyclic monophosphate in the apical membrane of *Necturus* enterocytes. *J. Physiol.* **344,** 000–027.

Gómez T., Badía P., Bolaños A. and Lorenzo A. (1986) Transport of galactose and sodium across lizard duodenum. *Comp. Biochem. Physiol.* **85A,** 103–107.

Grady G. F., Madoff M. A., Duhammel R. C., Moore E. Q. and Chalmers T. C. (1967) Sodium transport in human ileum *in vitro* and its response to cholera enterotoxin. *Gastroenterology* **53,** 737–744.

Grubb B. R., Driscoll S. M. and Bentley P. J. (1987) Electrical PD, short circuit current and fluxes of Na and Cl across avian intestine. *J. comp. Physiol.* **157, B** 181–186.

Gunter-Smith P. J., Grasset E. and Schultz S. G. (1982) Sodium-coupled amino acid and sugar transport by *Necturus* small intestine. *J. Membr. Biol.* **66,** 25–39.

Kaunitz J. D., Gunter R. and Wright E. M. (1982) Involvement of multiple sodium ions in intestinal D-glucose transport. Proc. natn Acad. Sci. USA **79,** 2315–2318.

Kimmich G. A. (1981) Intestinal absorption of sugar. In *Physiology of the Gastrointestinal Tract* (Edited by Johnson L., Christensen J., Grossman M., Jacobson E., and Schultz S.), pp. 1035–1061. Raven Press, New York.

Kimmich G. A. and Randles J. (1984) Sodium-sugar coupling stoichiometry in chick intestine cells. *Am. J. Physiol.* **247,** C74–C82.

Lamsfus C., Jordana R. and Ponz F. (1976) Active transport sugars in tortoise intestine. *Rev. Esp. Fisiol* **32,** 249–254.

Lorenzo A., Santana P., Gómez T. and Badía P. (1989) Sodium and chloride transport in the lizard duodenum. *Zool. Sci.* (in press).

Munck B. G. (1972) Effects of sugar and amino acid transport on transepithelial fluxes of sodium and chloride of short circuited rat jejunum. *J. Physiol.* **223,** 699–717.

Paterson J. Y. E., Sepulveda F. V. and Smith M. W. (1979) Two carrier influxes of neutral amino acids into rabbit ileal mucosa. *J. Physiol.* **292,** 339–350.

Rose R. C. and Schultz S. G. (1971) Studies on the electrical potential profile across rabbit ileum. Effects of sugars and

amino acids on transmural and transmucosal electrical potential differences. *J. gen. Physiol.* **57,** 639–663.

Suarez J. and Lorenzo A. (1982) Comparative studies on the transmural potential difference and the intensity of the short circuit current between the duodenum and the jejunum of the pigeon. *Rev. Esp. Fisiol.* **38,** 451–460.

Wright E. M. (1966) The origin of the glucose-dependent increase in the potential difference across the tortoise small intestine. *J. Physiol.* **185,** 486–500.